



**HAL**  
open science

## Medium effect on Cd3P2 quantum dots photoluminescence and addition of Pt nanoparticles: Inner filter effect and screening phenomena

Gaëlle Muraille, Simon Tricard, Edwin A Baquero, Benjamin Chekroun,  
Delphine Lagarde, Xavier Marie, Bruno Chaudret, Céline Nayral, Fabien  
Delpech

### ► To cite this version:

Gaëlle Muraille, Simon Tricard, Edwin A Baquero, Benjamin Chekroun, Delphine Lagarde, et al.. Medium effect on Cd3P2 quantum dots photoluminescence and addition of Pt nanoparticles: Inner filter effect and screening phenomena. *Journal of Luminescence*, 2020, 217, pp.116778. 10.1016/j.jlumin.2019.116778 . hal-02403293

**HAL Id: hal-02403293**

**<https://hal.insa-toulouse.fr/hal-02403293>**

Submitted on 21 Dec 2021

**HAL** is a multi-disciplinary open access archive for the deposit and dissemination of scientific research documents, whether they are published or not. The documents may come from teaching and research institutions in France or abroad, or from public or private research centers.

L'archive ouverte pluridisciplinaire **HAL**, est destinée au dépôt et à la diffusion de documents scientifiques de niveau recherche, publiés ou non, émanant des établissements d'enseignement et de recherche français ou étrangers, des laboratoires publics ou privés.



Distributed under a Creative Commons Attribution - NonCommercial 4.0 International License

# Medium effect on Cd<sub>3</sub>P<sub>2</sub> quantum dots photoluminescence and addition of Pt nanoparticles: inner filter effect and screening phenomena

*Gaëlle Muraille, Simon Tricard,\* Edwin A. Baquero, Benjamin Chekroun, Delphine Lagarde, Xavier Marie, Bruno Chaudret, Céline Nayral,\* and Fabien Delpech\**

*Laboratory:*

*<sup>1</sup>LPCNO; Laboratoire de Physique et Chimie de Nano-Objets*

*INSA, CNRS, Université de Toulouse*

*135, Avenue de Rangueil, 31077 Toulouse (France)*

*\*To whom correspondence should be addressed.*

E-mail: [cnayral@insa-toulouse.fr](mailto:cnayral@insa-toulouse.fr), [fdelpech@insa-toulouse.fr](mailto:fdelpech@insa-toulouse.fr), [tricard@insa-toulouse.fr](mailto:tricard@insa-toulouse.fr).

## **Abstract**

The formation of complex nanostructures combining quantum dots (QDs) and metallic nanoparticles (NPs) opens new perspectives to study and control energy transfer between them, provided that all the phenomena (reabsorption, screening and quenching effect) potentially affecting the photoluminescence (PL) of QDs could be identified and differentiated. First, dilution effect is studied on Cd<sub>3</sub>P<sub>2</sub> QDs and Cd<sub>3</sub>P<sub>2</sub>@ZnS core-shell QDs solutions. The full width at half maximum, the intensity and the emission wavelength are concentration-dependent, while the decay time of PL remains constant in the conditions of measurement. These effects are shown to be fully consistent with the so-called Inner Filter Effect. The addition of Pt NPs to the QD solution causes a clear decrease of the PL intensity which could be attributed to a screening of the emission of QDs by Pt NPs instead of a possible quenching due to an interaction between the two kinds of particles. Potential bias and experimental pitfalls are highlighted to avoid misleading PL interpretations.

## **Introduction**

Quantum dots (QDs) are promising objects due to their wide range of applications, ranging from light-emission to photodetection, solar cells, light emitting diode or tunable emitters for bio-labeling<sup>1-5</sup>. In the case of applications in solution (*i.e.* temperature probes, fluorescence resonance energy transfer, etc.), it is crucial to know the limiting conditions of use. Indeed, numerous parameters may affect the photoluminescence (PL) of QDs such as the concentration of ligands<sup>6-8</sup>, the dilution<sup>9,10</sup>, the presence of other chemical compounds<sup>11-13</sup>, and may hinder the use of fluorescence properties as a quantitative tool. In particular, the consequences of the Inner-Filter Effect (IFE) have to be seriously taken into account to avoid misleading interpretations<sup>14,15</sup>. This concentration-dependent effect can be described as the combination of: (i) a Primary Inner Filter Effect (PIFE) due to the fact that concentrated solutions act as a real filter preventing light going through the solution, and (ii) a Secondary Inner Filter Effect (SIFE) due to the possible reabsorption of the emitted light by the solution. When the concentration is high enough, IFE results in a decrease of the luminescence intensity compared to more diluted samples. SIFE occurs when the absorbance of the sample overlaps its luminescence. The QD absorption in the emission range then implies a decrease of the luminescence intensity, and thus a distortion of the band shape. Indeed, the emission of given QDs can be reabsorbed by other QDs with a lower energy band gap (larger ones), which can then subsequently undergo radiative transition (and emit lower energy photons) or non-radiative relaxation. This phenomenon leads to an apparent decrease of the emission of the smaller QDs (at higher energy) and an increase of the emission of the larger ones (at lower energy). As a result, in presence of SIFE, the global PL emission wavelength is red-shifted while the QD concentration

increases. Even if such effects are sometimes considered as “obvious”, very few systematic studies have been carried out in depth<sup>7-9</sup>. We can mention the works of Zhang et al.<sup>16</sup> on colloidal carbon QD solutions or of Mei et al. on solutions of ZnSe QDs<sup>9</sup>, this latter evidencing that the optimal QD density to maximize the PL intensity was related to QD spacing and thus to the QD size. More recently, Noblet et al.<sup>14</sup> investigated the concentration effect on CdTe QD solutions to develop a model based on the IFE. They demonstrate that the concentration dependent behaviour of QD fluorescence can be fully understood by the IFE, precluding any hypothesis of dynamic quenching. Despite reabsorption is generally considered as limiting<sup>15,17</sup>, some recent studies take advantage of reabsorption appearing at high concentrations to build optical sensors based on the IFE<sup>18,19</sup>, which requires then a deep understanding of this effect for the optimization of such systems<sup>20</sup>.

A current concern focuses on combining QDs and metallic nanoparticles (NPs) to study energy transfer between them<sup>13,21-23</sup>. The goal of such an approach would be to control the transfer of the exciton – generated by light absorption in the QDs – or of the excited electron or hole from the QDs to the NPs, by a suitable engineering of the relative energy levels. QDs would act as antennas to harvest light energy and thus activate the physical or chemical activity of NPs, *e.g.* in charge transport or catalysis. A challenge in this field is to overcome the low energy transfer efficiency from or to the QDs due to their small size<sup>24</sup>. In solution, a simple dilution can affect the PL of QDs, by lowering the concentration of ligands, of quenchers and increasing the distance between objects. It is thus crucial to precisely know phenomena affecting the PL of QDs and to differentiate reabsorption, screening and quenching effect.

We have chosen to study the combination of platinum (Pt) NPs and cadmium phosphide ( $\text{Cd}_3\text{P}_2$ ) QDs.  $\text{Cd}_3\text{P}_2$  is an interesting material because of its small band gap of 0.55 eV (at 300 K)<sup>25</sup> and its large exciton Bohr radius (18 nm), which make it suitable for systems emitting from the visible to the near infrared<sup>26-28</sup>, including the whole sunlight range of emission. Ultra-small (< 2 nm) Pt NPs are air stable and have demonstrated to show Coulomb blockade at room temperature, phenomenon that makes them promising nanoelectrodes to study charge transport at the nanoscale<sup>29</sup>.

In this context, we first present the reabsorption effect of  $\text{Cd}_3\text{P}_2$  QDs and  $\text{Cd}_3\text{P}_2$ @ZnS core-shell QDs. The consequence of addition of Pt NPs on the PL of  $\text{Cd}_3\text{P}_2$  QDs is then investigated.

## **Experimental method**

**Materials:** Cadmium acetate ( $\text{Cd}(\text{OAc})_2$ ,  $\geq 99.99\%$ ), octylamine ( $\geq 99.0\%$ ), tris(dibenzylideneacetone)diplatinum(0) ( $\text{Pt}_2(\text{dba})_3$ ,  $\geq 98.0\%$ ) and tris(trimethylsilyl)phosphine ( $(\text{TMS})_3\text{P}$ ,  $\geq 98.0\%$ ) were purchased from Strem, ethylene sulphide ( $\text{C}_2\text{H}_4\text{S}$ ,  $\geq 98.0\%$ ), hexadecylamine ( $\text{C}_{16}\text{H}_{35}\text{N}$ ,  $\geq 98.0\%$ ) and pentane ( $\text{CH}_3(\text{CH}_2)_3\text{CH}_3$ ,  $\geq 98.0\%$ ) were purchased from Aldrich. Ethanol (EtOH), tetrahydrofuran (THF) and toluene (RPE, Analysis grade) were purchased from Carlo Erba. Ethanol and toluene were dried and degassed before use. All manipulations were carried out under argon atmosphere using Schlenk tubes and vacuum line techniques or in glovebox with anhydrous solvent purged under argon before using.

**Synthesis of  $\text{Cd}_3\text{P}_2$  QDs:** In a typical low-temperature synthesis, 0.692 g (3.0 mmol) of  $\text{Cd}(\text{OAc})_2$  and 1.702 g (7.05 mmol) of hexadecylamine were mixed with 8 mL of toluene and loaded into a 50 mL three-necked flask. The solution was heated to  $35^\circ\text{C}$  and 2 mL of a  $(\text{TMS})_3\text{P}$  solution ( $0.5 \text{ mol}\cdot\text{L}^{-1}$  in toluene, 1 mmol) was injected. After injection the colour of the solution changed from yellow to battle-grey. The reaction was maintained at  $35^\circ\text{C}$  for 20h. The same protocol is used to form  $\text{Cd}_3\text{P}_2$ @octylamine taking octylamine instead of hexadecylamine with the same ratio.

**Synthesis of  $\text{Cd}_3\text{P}_2$ @ZnS QDs:** In a typical low-temperature synthesis, 5 mL of  $\text{Cd}_3\text{P}_2$  QDs ( $0.125 \text{ mmol}$  based on P) and 165.3 mg ( $0.3740 \text{ mmol}$ ) of freshly prepared zinc acetate dioctylamine ( $\text{Zn}(\text{OAc})_2(\text{OAm})_2$ ) in 3.9 mL of toluene were mixed and loaded into a 50 mL three-necked flask. The solution was heated to  $35^\circ\text{C}$  and 1.10 mL of ethylene sulfide solution ( $0.36 \text{ mol}\cdot\text{L}^{-1}$  in toluene,  $0.369 \text{ mmol}$ ) was injected. The reaction was maintained at  $35^\circ\text{C}$  for 20h. After, the solution was kept in the glovebox at  $-30^\circ\text{C}$ . The same procedure is used to shell either  $\text{Cd}_3\text{P}_2$ @octylamine or  $\text{Cd}_3\text{P}_2$ @hexadecylamine.

**Synthesis of Pt nanoparticles:** a solution of tris(dibenzylideneacetone)diplatinum(0) in tetrahydrofuran (THF) at 4.12 mM is prepared and introduced in a fisher-porter. Then a pressure of 1 bar of carbon monoxide (CO) is applied for 3 min. After that, the fisher-porter is closed and left under magnetic stirring for 30 min. The THF is evaporated and 15 mL of pentane is added under vigorous stirring. The magnetic stirring is stopped after a few minutes and the nanoparticles precipitate. The supernatant is removed and 3 mL of THF is added under stirring. This washing step is repeated twice.

**Addition of Pt nanoparticles:** The QDs were first dried from toluene solution and then dispersed in THF. Solutions with different QDs/Pt NPs ratios are obtained by adding different concentrations of Pt NPs and keeping the same concentration of QDs, in THF. A solution of pure QDs is prepared in the same way (ratio 1:0) in order to be able to compare properly.

### **Samples characterization**

**TEM analysis:** samples for TEM analysis were prepared by evaporation of a drop of the colloidal solution deposited onto a carbon-covered copper grid. TEM analysis were performed at the “Centre de MicroCaractérisation Raimond Castaing” on a JEOL JEM 1400 electron microscope operating at 120kV with a point resolution of 4.5 Å. The size distributions were determined by measuring by hand the diameter of ca. 320 particles using Image J software. The mean diameter and the standard deviation are calculated from these values.

**UV-Visible Absorption measurement:** absorbance spectra were measured in solution by using a Perkin Elmer lambda 35 scanning spectrometer with 2 mm-wide cells.

**Photoluminescence (PL) measurement:** continuous wave cw-PL spectra were recorded in solution using a xenon lamp as excitation source. The white light is dispersed by a monochromator and filtered at 500 nm. The PL emission is collected at 90° with respect to the excitation beam, dispersed by a monochromator and recorded using a UV-vis Hamamatsu photomultiplier tube. Acquisition is performed by the FelixGX software and all the spectra were recorded with the same parameters. The detection range is limited to wavelengths below 800 nm, so the signal cannot be detected entirely for several solutions. In order to determine the full width at half maximum (FWHM), the curves were fitted with the GaussAmp function of Origin, the correlation coefficient was checked for each curve ( $R^2 > 0.995$ ).

**Determination of absolute quantum yield:** Quantum yield measurements were performed at room temperature using an integrating sphere (Labsphere). The calculations were performed following a procedure already reported<sup>30</sup>. Briefly the quantum yield was calculated as the ratio of the number of emitted photons and the number of absorbed photons: the number of emitted photons was obtained by subtracting the signal of the solvent to the signal of the sample in the range of emission and by integrating the resulting signal. The number of absorbed photons was obtained by subtracting the signal of the solvent to the signal of the sample around the peak of excitation and by integrating it. The luminescence parts of the curves were fitted with a GaussAmp function on Origin software before the calculation of the integrated emission.

**Time-resolved photoluminescence (TRPL) experiments:** TRPL spectra were performed at room temperature using a mode-locked frequency-doubled Ti-sapphire laser with a 1.5 ps pulse width and a wavelength of 430 nm. A pulse picker was used to reduce the repetition rate from 80 MHz to 0.4 MHz. The non-resonant TRPL is dispersed by a spectrometer and then recorded using a

Hamamatsu S20 photocathode streak camera with an overall temporal resolution of  $\sim 50$  ns. The excitation average power is kept at  $\sim 20 \mu\text{W}$  @ 0.4 MHz with a laser spot diameter of  $\sim 2$  mm.

## **Results and discussion**

The evolution of PL with the concentration has been investigated on  $\text{Cd}_3\text{P}_2$  and  $\text{Cd}_3\text{P}_2@\text{ZnS}$  QDs, synthesized accordingly to published protocols<sup>31</sup>. Transmission electron microscopy (TEM) images of the samples are shown in Figure 1. The mean diameter of the roughly spherical particles is centred around 2.6 nm (standard deviation SD  $\pm 0.7$  nm) for the cores and 3.6 nm (SD  $\pm 0.9$  nm) for the shelled QDs.

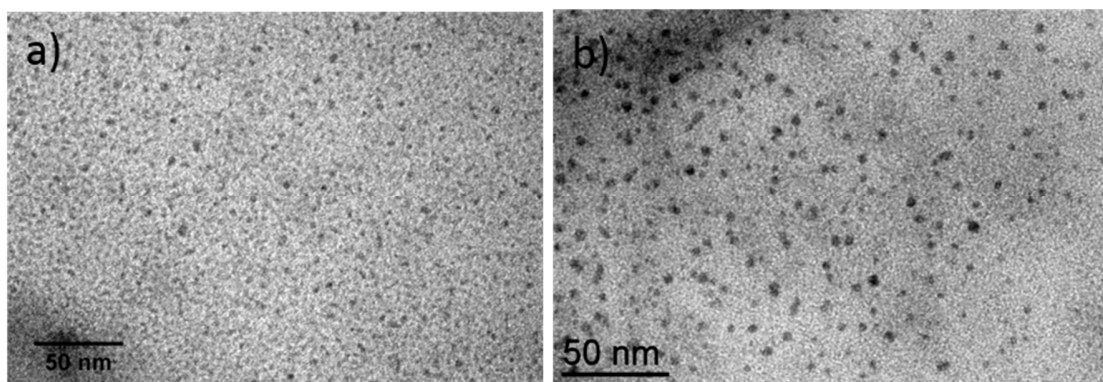


**Figure 1. TEM images of a)  $\text{Cd}_3\text{P}_2$  and b)  $\text{Cd}_3\text{P}_2@\text{ZnS}$**

The QD concentration effect is studied by preparing a set of successive diluted samples. The concentration of the samples is expressed on the basis of the introduced  $(\text{TMS})_3\text{P}$  which is the limiting agent (the concentrations of  $(\text{TMS})_3\text{P}$ , going from 18.8 to 0.10  $\text{mmol}\cdot\text{L}^{-1}$ , are given in Table 1 from C1 to C18). The optical absorption at 500 nm, chosen as a concentration marker, has been systematically measured and reported (see Table 1). All graphs depending on the

concentration presented in this paper are traced as a function of absorbance. The range of application of the Beer-Lambert law is limited to the very low concentrations, from C9 to C18 (see Figure S1).

**Table 1. Corresponding concentrations of (TMS)<sub>3</sub>P/2 with the absorbance at 500 nm**

Notation	Corresponding concentration of (TMS) <sub>3</sub> P/2 (mmol.L <sup>-1</sup> )	Absorbance at 500 nm
C1	18.8	4.3
C2	12.5	3.6
C3	9.38	2.7
C4	6.26	1.9
C5	4.69	1.5
C6	3.13	1.2
C7	2.35	0.83
C8	1.56	0.65
C9	1.17	0.55
C10	0.98	0.45
C11	0.78	0.35
C12	0.69	0.30
C13	0.59	0.25
C14	0.49	0.19
C15	0.39	0.13
C16	0.29	0.10
C17	0.20	0.06
C18	0.10	0.03

### Dilution study

First of all, the integrity of the Cd<sub>3</sub>P<sub>2</sub> QDs in solution and upon dilution has been investigated (C1, the stock solution of Cd<sub>3</sub>P<sub>2</sub> QDs, is diluted up to a factor of 188 to obtain the sample C18). Absorption spectra are presented in Figure S2a. The absorbance decreases upon dilution as expected, and normalized absorption spectra at the different concentrations overlap perfectly (Figure S2b). The constant shape of the absorption spectrum upon dilution indicates that the size distribution of the QDs is unmodified, and thus their integrity preserved.

Continuous wave (cw)-PL spectra of solutions of Cd<sub>3</sub>P<sub>2</sub> QDs at the different concentrations are presented in Figure 2a. Upon dilution, fluorescence spectra exhibit a shape significantly dependent to concentration. The PL intensity first increases to reach a maximum for C6 and then decreases (Figure S3). For sake of clarity, absorption and PL spectra of three different concentrations are traced in Figure 2b, evidencing the overlap between absorption and emission. The small Stokes shift comes from reabsorption phenomena (SIFE), since the emission of the smallest QDs can be reabsorbed by the largest ones. Upon dilution, this results in a blue-shift of ~ 55 nm (from 770 to 715 nm) within the range of the considered concentrations (Figure 2c) while at the same time, the FWHM increases from 62 to reach a maximum at 87 nm (Figure 2d).

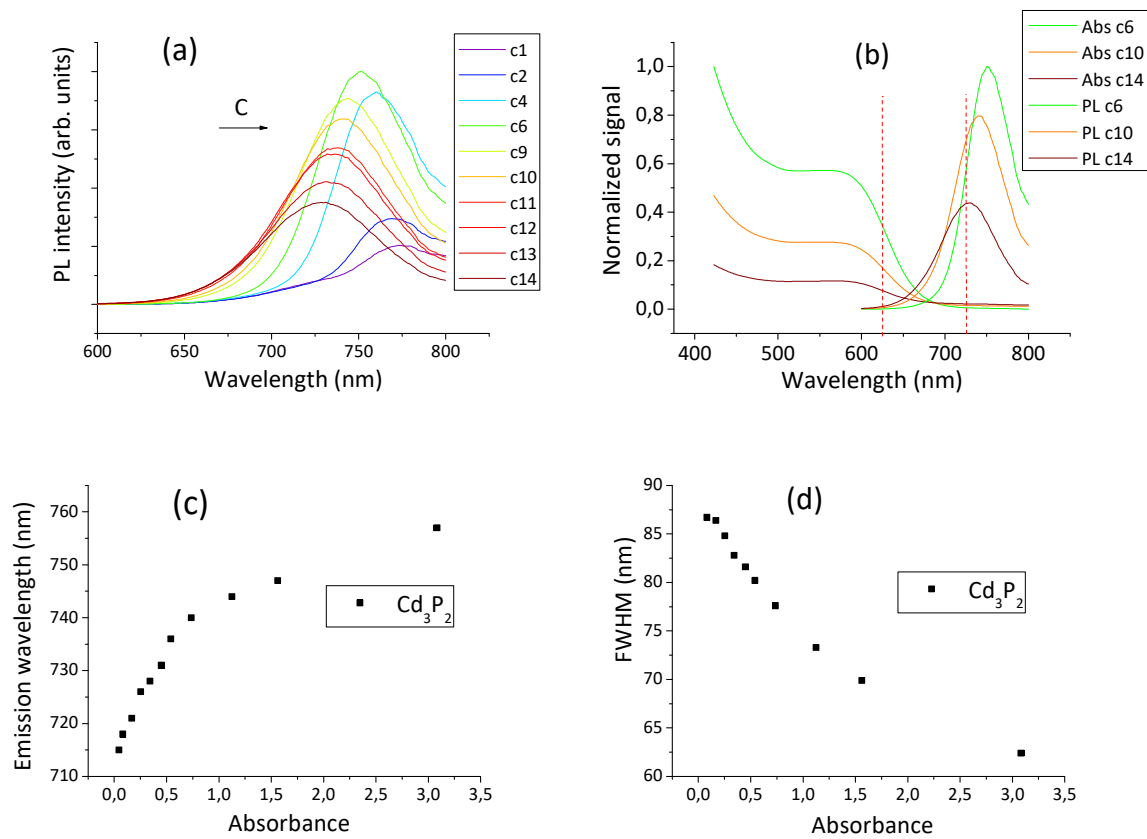


**Figure 2. a) PL spectra of Cd<sub>3</sub>P<sub>2</sub>@HDA – b) Normalized PL and absorption spectra of Cd<sub>3</sub>P<sub>2</sub>@HDA, red vertical dashed lines represent the overlap zone – c) Evolution of the FWHM as a function of the absorbance at 500nm and – d) Evolution of the emission wavelength (for the same concentrations as presented on (b))**

The impact of the reabsorption on the FWHM is of main importance because this value is commonly used to evaluate the size-dispersity of suspensions of QDs<sup>4,34,35</sup>. However, the correlation between the FWHM and the size distribution can be applied only when using highly diluted solutions. The same argumentation is valuable for the PL emission wavelength (Figure 2c). These values are representative of the sample only when the SIFE is avoided. Concerning Cd<sub>3</sub>P<sub>2</sub> QDs, the emission wavelength indeed continues to decrease upon dilution even for highly diluted solutions, showing that IFE are still present at such concentrations. Unfortunately, it was not possible to measure significant signal in absorbance and PL anymore with the same

acquisitions parameters at more diluted solution. Cd<sub>3</sub>P<sub>2</sub> QDs show such strong IFE that it was not possible to observe any concentration range where the FWHM and the emission wavelength is stabilized.

TRPL measurements (Figure 3) provide information on the temporal evolution of the optical transitions. Contrary to what observed in cw-PL experiments (Figure 2a), a linear decrease of the time-integrated PL intensity upon dilution is observed while the emission wavelength remains stable, the slight blue-shift observed between C3 and C8 is not significant in TRPL (Figure 3a).

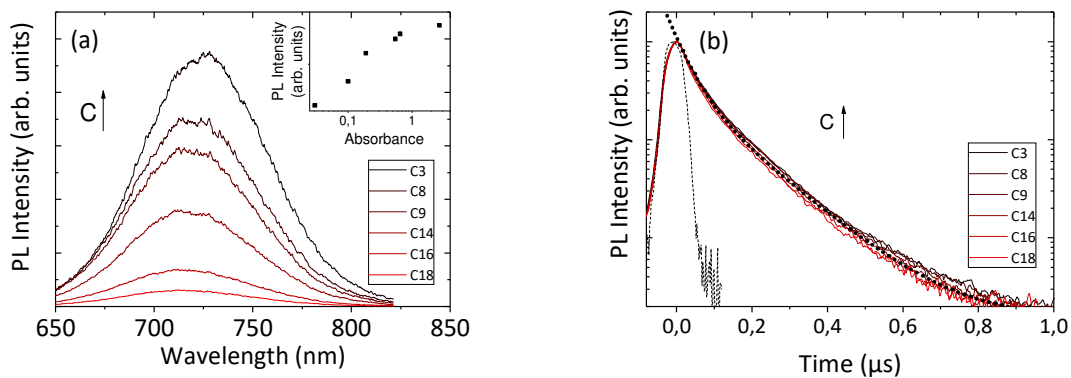


**Figure 3. a) Time-integrated TRPL spectra of Cd<sub>3</sub>P<sub>2</sub>@hexadecylamine Inset: Evolution of total PL Intensity as a function of absorbance – b) PL dynamics of Cd<sub>3</sub>P<sub>2</sub>@hexadecylamine integrated over the full spectral range at several concentrations. The dashed curve shows the instrument response function of the detection apparatus and the dotted line the bi-exponential fit of the TRPL decay**

The normalized PL dynamics spectra at different concentrations are presented on Figure 3b, integrated over the full spectral range. The fluorescence decay curve of Cd<sub>3</sub>P<sub>2</sub> is fitted by a bi-exponential decay curve and two characteristic times were obtained:  $t_1 \sim 40$  ns and  $t_2 \sim 135$  ns. The shorter lifetime could be attributed to the intrinsic recombination of the electron-hole pair of the core and the longer one to the presence of trapped carriers at the surface<sup>6,32,33</sup>. No

significant change of the rise or decay time values has been observed with the QD concentration within the temporal resolution of our setup ( $\sim 50$  ns). Note that furthermore both rise and decay times do not evolve as a function of the detection wavelength. The ratio of the emission coming from the cores and from the surface defects thus remains constant upon dilution. The absence of lifetime evolution confirms the stability of the QDs in solution (no modification of size or of surface states) on the range of the studied concentrations. A blue shift due to the SIFE was clearly evidenced in stationary experiments while it was not detectable in TRPL experiments. We assume that the reabsorption phenomena are not efficient enough as the overall QDs population is still in a bleach state during most of the emission lifetime. Transient absorption measurements have indeed demonstrated that exciton bleach recovery in II-VI QDs occurs in similar time scale as the PL decay time measured here ( $\approx 135$  ns)<sup>36</sup>.

Luminescence spectra of different dilutions of core-shell QDs are recorded under the same conditions as mentioned above. The spectra are presented in Figure S4a, and the evolution of the maximum PL intensity of both, core and core-shell QDs, is presented in Figure S4b. The core-shell system exhibits the same behavior as the  $\text{Cd}_3\text{P}_2$  cores: upon dilution, the intensity first increases and then decreases. The evolutions of the absorption spectra (see Figure S5), of the emission wavelength (Figure 4a) and of the FWHM (Figure 4b) show the same trend as for the  $\text{Cd}_3\text{P}_2$  cores. The emission wavelength blue-shift, between the highest and lowest concentration of  $\text{Cd}_3\text{P}_2@ZnS$ , is evaluated to  $\sim 50$  nm. The shape of absorption spectra remains unchanged upon dilution, indicating that the average size and the size distribution of the QDs are stable (see Figure S5).

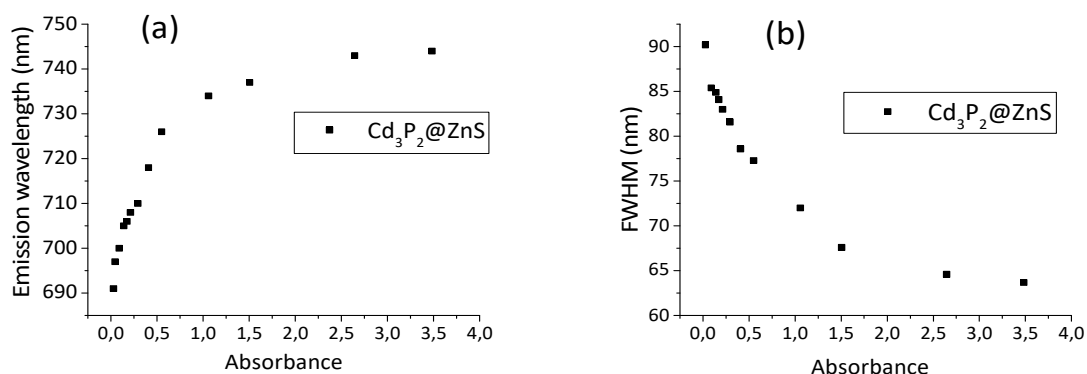


**Figure 4. a) Evolution of the emission wavelength and b) Evolution of the FWHM of Cd<sub>3</sub>P<sub>2</sub> and Cd<sub>3</sub>P<sub>2</sub>@ZnS upon dilution**

TRPL decay times were found to be around 60-90 ns for the shorter and 185-215 ns for the longer ones, in the same range as the ones measured on the uncoated cores (see Figure S4). The slight change of decay time upon dilution is not significant, which indicates that the optical transitions do not change.

These results show that reabsorption occurs in a similar manner compared to the core only and that the modification behaviour of the PL emission spectrum features (wavelength, FWHM, intensity) can be fully explained by the IFE phenomenon. A concentration range without reabsorption has not been reached here neither. A plateau where IFE are negligible should be reached at lower dilution, but too low to detect any PL or UV/Vis absorption signal with common experimental apparatus.

### Quenching and screening effect

Recent reports focus on hybrid structures to study the energy exchange between two different kinds of nanoparticles<sup>13,21-23</sup>. In this context, Pt NPs were chosen as model systems to form mixed assemblies of metallic NPs with Cd<sub>3</sub>P<sub>2</sub> QDs. A process where Pt NPs (~1-3 nm) are naked

(i.e. only stabilized by the solvent THF, and by carbon monoxide coming from the synthesis process) was used<sup>37</sup>. The interest of such naked NPs is the absence of extra ligands; we are thus completely sure that no exchange phenomena will compete with the octylamine ligand stabilizing the QDs, which will thus remain chemically unmodified – excess of octylamine from the QD solution will probably coordinate to the Pt surface. Pt NPs were added to Cd<sub>3</sub>P<sub>2</sub> QDs stabilized with octylamine at different ratios. A solution of QDs with an absorbance of 0.1 was prepared, thus fixing the concentration of QDs. The concentration of the Pt NPs varied to obtain different QDs: Pt NPs ratios (1:0 – 1:0.1 – 1:1 – 1:10). The ratios correspond to the molar ratios Cd<sub>3</sub>P<sub>2</sub>:Pt, taking into account the quantity of introduced (TMS)<sub>3</sub>P/2 – which is the limiting agent for the Cd<sub>3</sub>P<sub>2</sub> QD synthesis – and the quantity of introduced Pt atoms. TEM images were realized to check the homogeneity of these different mixtures (Figure 5). For all ratios, both the QDs and the Pt NPs are well dispersed and uniformly mixed.

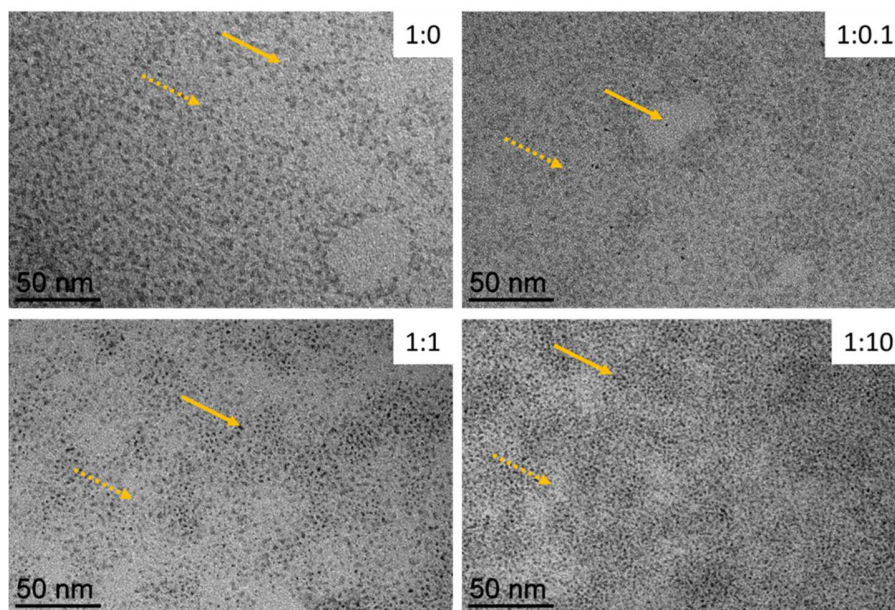


**Figure 5. TEM images of  $\text{Cd}_3\text{P}_2$  and Pt NPs (ratio  $\text{Cd}_3\text{P}_2$ :Pt NPs): Pt NPs present a higher contrast than  $\text{Cd}_3\text{P}_2$  QDs and appear as dark small spots on the images (examples shown by plain arrows), whereas  $\text{Cd}_3\text{P}_2$  QDs appear as larger grey spots (examples shown by dashed arrows)**

To study the effect of the Pt NPs on the optical properties of QDs, absorption spectra of the different mixtures were measured and are presented in Figure S7. The broad peak around 600 nm related to the QDs (curve 1:0) disappears progressively with the addition of Pt NPs while the absorbance at higher energies increases. PL intensity and quantum yield of mixtures were measured (Figure 6). They both decrease to be null at a ratio of 1:10 so the presence of Pt NPs implies a decrease of the QDs fluorescence. The question is thus now to determine if the loss of PL intensity is the consequence of a quenching by Pt NPs, or the result of a screening by the metallic NPs.

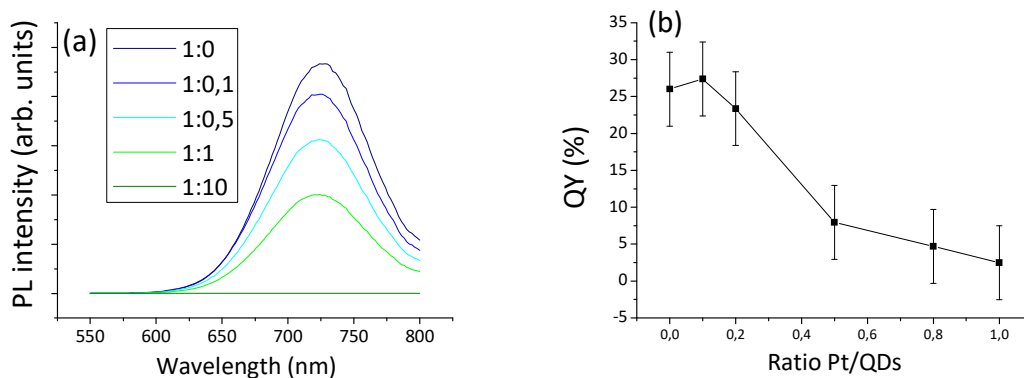


**Figure 6. a) PL spectra and b) Quantum yield of mixtures of Cd<sub>3</sub>P<sub>2</sub> and Pt NPs**

Two main types of quenching are known: the static and the dynamic quenchings. A dynamic quenching would result from the collision of the QDs at the excited state with the Pt NPs, which would lead to a charge or energy transfer. A static quenching would come from the formation of a new not-luminescent compound resulting from the interaction between the QDs and the Pt NPs at their fundamental state. In the case of dynamic quenching, the decay time would be affected by the concentration of Pt NPs because quenching depopulates the excited states. PL dynamics spectra show that no modification of the decays is observed for the mixtures with different ratios of QDs and Pt NPs (Figure 7). The curves can be fitted by a bi-exponential decay, the longest decay time was found equal to 190 ns and the shortest to 90 ns. These values are similar to those for the QDs alone, without Pt NPs. The optical transitions of the QDs are thus not modified by the presence of Pt NPs. Dynamic quenching is therefore excluded. Two hypotheses remain to explain the loss of intensity observed after addition of Pt NPs: a static quenching or just a screening of Pt NPs without any interaction between QDs and NPs.

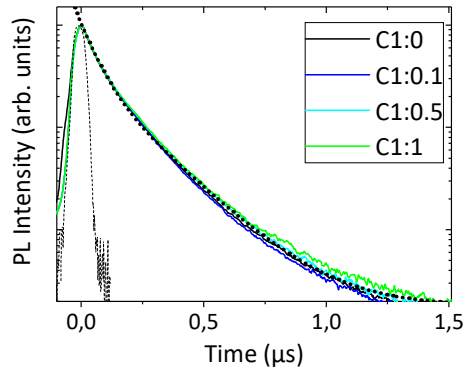


**Figure 7. TRPL measurements for mixtures of  $\text{Cd}_3\text{P}_2$  and Pt NPs integrated over the all spectrum. The dashed and dotted lines correspond to the instrument response function of the apparatus and the bi-exponential fit of the decay, respectively**

In the case of static quenching, a complex is formed at the fundamental state. This complex should have a different absorption than the addition of Pt NPs alone and of QDs alone. On Figure 8 absorption spectra of Pt NPs (0:1), of QDs (1:0), of the mixture (1:1) and of the mathematical addition (0:1 + 1:0) of the Pt NP and QD signals are presented.

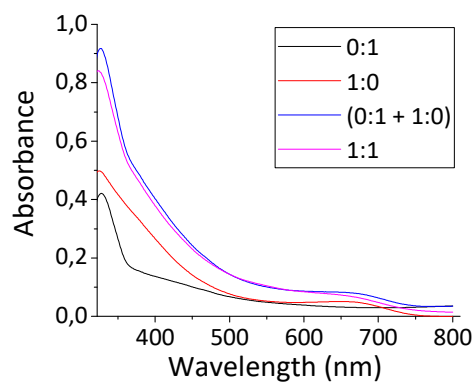


**Figure 8. Absorption spectrum of Pt NPs (0:1), of QDs (1:0), of the mixture of NPs and QDs (1:1) and of the mathematical addition of absorption spectra of NPs and QDs (0:1 + 1:0)**

The absorption spectra of the mixture and the mathematical addition of independent spectra have the same trend and superimpose almost perfectly. This observation does not evidence the formation of a complex at the fundamental state. In this particular case, no specific interaction is demonstrated between the Pt NPs and the QDs, so that neither dynamic nor static quenching can be stated. The decrease of luminescence is most probably the consequence of absorption of the incident and emitted light by the Pt NPs. This demonstration aims at warn the community that a decrease of QDs luminescence by the addition of a coproduct in solution is not necessarily the consequence of a quenching effect. Indeed, one should always double-check first that it is not the result of a simple screening effect, which is not systematically done in every article.

## **Conclusion**

As a conclusion, the IFE explains the behaviour of the PL upon dilution of  $\text{Cd}_3\text{P}_2$  and  $\text{Cd}_3\text{P}_2@\text{ZnS}$  QDs solutions. A systematic study has never been performed on such QD so far. For each type of QDs, the FWHM, the intensity and the emission wavelength are concentration-dependent, while the decay time of PL remains constant in our measurements conditions. The characteristics of the IFE upon dilution are first an increase and then a decrease of the PL intensity, a blue-shift of the emission wavelength and a widening of the FWHM. As a consequence, in such a case, the maximum PL intensity is not representative of the emitting core size and the FWHM is not representative of the size distribution at any concentration. Concerning the mixture of Pt NPs and  $\text{Cd}_3\text{P}_2$  QDs, the decrease of the PL intensity by adding Pt NPs is not caused by a quenching but by a simple screening of the emission of QDs by Pt NPs. In a nutshell, this report stresses that PL measurements can give important information on the nature of a colloidal suspension, but one should be aware that several experimental pitfalls can be encountered on PL interpretation: reabsorption for a FWHM narrowing and not a narrower size distribution, reabsorption for a blue-shift and not a size decrease, reabsorption for an intensity decrease and not a QD denaturation, reabsorption for a shift in emission wavelength after shelling and not a decrease of the core size, screening effect for a co-product addition and not a quenching effect. Ideally, concentration of the QDs is such an important parameter for PL measurements that information about suitable concentrations for spectral testing should be systematically investigated in any study. Taking all these considerations into account,  $\text{Cd}_3\text{P}_2$  QDs are promising elements for using luminescence as a tool for studying response to external parameters (light,

temperature, chemical compounds, etc.), if they are studied in proper conditions, being aware of the previous limitations. Experiments in that sense are currently under investigation.

## **Acknowledgments**

This work was supported by the Université Paul Sabatier, the Région Occitanie, the CNRS, the Institut National des Sciences Appliquées of Toulouse, the Programme Investissements d'Avenir under the program ANR-11-IDEX-0002-02, reference ANR-10-LABX-0037-NEXT, and the European Commission for ERC Grant No GA694159 – MONACAT. E.A.B. is grateful to Marie Curie Actions and Campus France for a PRESTIGE post-doc fellowship (FP7/2007–2013) under REA grant agreement no. PCOFUND-GA-2013-609102.

## **References:**

- <sup>1</sup> D.V. Talapin, J.-S. Lee, M.V. Kovalenko, and E.V. Shevchenko, *Chem. Rev.* **110**, 389 (2010).
- <sup>2</sup> R. Xie, D. Battaglia, and X. Peng, *J. Am. Chem. Soc.* **129**, 15432 (2007).
- <sup>3</sup> D. Onoshima, H. Yukawa, and Y. Baba, *Adv. Drug Deliv. Rev.* **95**, 2 (2015).
- <sup>4</sup> J.M. Pietryga, Y.-S. Park, J. Lim, A.F. Fidler, W.K. Bae, S. Brovelli, and V.I. Klimov, *Chem. Rev.* **116**, 10513 (2016).
- <sup>5</sup> Y. Cao, A. Stavrinadis, T. Lasanta, D. So, and G. Konstantatos, *Nat. Energy* **1**, 16035 (2016).
- <sup>6</sup> M. Greben, A. Fucikova, and J. Valenta, *J. Appl. Phys.* **117**, 144306 (2015).
- <sup>7</sup> L. Hartmann, A. Kumar, M. Welker, A. Fiore, C. Julien-Rabant, M. Gromova, M. Bardet, P. Reiss, P.N.W. Baxter, F. Chandezon, and R.B. Pansu, *ACS Nano* **6**, 9033 (2012).
- <sup>8</sup> A.M. Munro, I. Jen-La Plante, M.S. Ng, and D.S. Ginger, *J. Phys. Chem. C* **111**, 6220 (2007).
- <sup>9</sup> B.C. Mei, J. Wang, Q. Qiu, T. Heckler, A. Petrou, and T.J. Mountziaris, *Appl. Phys. Lett.* **93**, 083114 (2008).
- <sup>10</sup> M. Kubista, R. Sjöback, S. Eriksson, and B. Albinsson, *Analyst* **119**, 417 (1994).
- <sup>11</sup> M.S. Hosseini and A. Pirouz, *Luminescence* **29**, 798 (2014).
- <sup>12</sup> D. Kim, H. Yokota, T. Taniguchi, and M. Nakayama, *J. Appl. Phys.* **114**, 154307 (2013).
- <sup>13</sup> P. Viste, J. Plain, R. Jaffiol, A. Vial, P.M. Adam, and P. Royer, *ACS Nano* **4**, 759 (2010).
- <sup>14</sup> T. Noblet, L. Dreesen, J. Hottechamps, and C. Humbert, *Phys Chem Chem Phys* **19**, 26559 (2017).
- <sup>15</sup> S. Fery-Forgues and D. Lavabre, *J. Chem. Educ.* **76**, 1260 (1999).
- <sup>16</sup> W. Zhang, D. Dai, X. Chen, X. Guo, and J. Fan, *Appl. Phys. Lett.* **104**, 091902 (2014).

- <sup>17</sup> M.A. Koc, S.N. Raja, L.A. Hanson, S.C. Nguyen, N.J. Borys, A.S. Powers, S. Wu, K. Takano, J.K. Swabeck, J.H. Olshansky, L. Lin, R.O. Ritchie, and A.P. Alivisatos, *ACS Nano* **11**, 2075 (2017).
- <sup>18</sup> Q.Q. Zhang, B.B. Chen, H.Y. Zou, Y.F. Li, and C.Z. Huang, *Biosens. Bioelectron.* **100**, 148 (2018).
- <sup>19</sup> S. Chen, Y.-L. Yu, and J.-H. Wang, *Anal. Chim. Acta* **999**, 13 (2018).
- <sup>20</sup> M. Ganiga, N.P. Mani, and J. Cyriac, *ChemistrySelect* **3**, 4663 (2018).
- <sup>21</sup> N. Mondal and A. Samanta, *J. Phys. Chem. C* **120**, 650 (2016).
- <sup>22</sup> U. Uddayasankar and U.J. Krull, *Langmuir* **31**, 8194 (2015).
- <sup>23</sup> H. Han, V. Valle, and M.M. Maye, *J. Phys. Chem. C* **116**, 22996 (2012).
- <sup>24</sup> A.R. Clapp, I.L. Medintz, J.M. Mauro, B.R. Fisher, M.G. Bawendi, and H. Mattoussi, *J. Am. Chem. Soc.* **126**, 301 (2004).
- <sup>25</sup> A. Nayak and D.R. Rao, *Appl. Phys. Lett.* **63**, 592 (1993).
- <sup>26</sup> R. Xie, J. Zhang, F. Zhao, W. Yang, and X. Peng, *Chem. Mater.* **22**, 3820 (2010).
- <sup>27</sup> S. Miao, S.G. Hickey, B. Rellinghaus, C. Waurisch, and A. Eychmüller, *J. Am. Chem. Soc.* **132**, 5613 (2010).
- <sup>28</sup> R. Wang, C.I. Ratcliffe, X. Wu, O. Voznyy, Y. Tao, and K. Yu, *J. Phys. Chem. C* **113**, 17979 (2009).
- <sup>29</sup> S. Tricard, O. Said-Aizpuru, D. Bouzouita, S. Usmani, A. Gillet, M. Tassé, R. Poteau, G. Viau, P. Demont, J. Carrey, and B. Chaudret, *Mater. Horiz.* **4**, 487 (2017).
- <sup>30</sup> C. Würth, M. Grabolle, J. Pauli, M. Spieles, and U. Resch-Genger, *Nat. Protoc.* **8**, 1535 (2013).
- <sup>31</sup> W.-S. Ojo, S. Xu, F. Delpech, C. Nayral, and B. Chaudret, *Angew. Chem. Int. Ed.* **51**, 738 (2012).
- <sup>32</sup> E.V. Ushakova, A.P. Litvin, P.S. Parfenov, A.V. Fedorov, M. Artemyev, A.V. Prudnikau, I.D. Rukhlenko, and A.V. Baranov, *ACS Nano* **6**, 8913 (2012).
- <sup>33</sup> X. Wang, L. Qu, J. Zhang, X. Peng, and M. Xiao, *Nano Lett.* **3**, 1103 (2003).

<sup>34</sup> C. de Mello Donegá, S.G. Hickey, S.F. Wuister, D. Vanmaekelbergh, and A. Meijerink, *J. Phys. Chem. B* **107**, 489 (2003).

<sup>35</sup> H. Zhang, L. Wang, H. Xiong, L. Hu, B. Yang, and W. Li, *Adv. Mater.* **15**, 1712 (2003).

<sup>36</sup> Shengye Jin, Jung-Cheng Hsiang, Haiming Zhu, Nianhui Song, Robert M. Dicksonb and Tianquan Lian, *Chem. Sci.* **1**, 519 (2010)

<sup>37</sup> F. Dassenoy, K. Philippot, T. Ould Ely, C. Amiens, P. Lecante, E. Snoeck, E. Mosset, M.-J. Casanove, and B. Chaudret, *New J. Chem.* 703 (1998).

# Medium effect on Cd<sub>3</sub>P<sub>2</sub> quantum dots photoluminescence and addition of Pt nanoparticles: inner filter effect and screening phenomena

## Supporting Information

*Gaëlle Muraille, Simon Tricard,\* Edwin A. Baquero, Benjamin Chekroun, Delphine Lagarde, Xavier Marie, Bruno Chaudret, Céline Nayral,\* and Fabien Delpech\**

*Laboratories:*

*<sup>1</sup>LPCNO; Laboratoire de Physique et Chimie de Nano-Objets*

*INSA, CNRS, Université de Toulouse*

*135, Avenue de Rangueil, 31077 Toulouse (France)*

*\*To whom correspondence should be addressed.*

*E-mail: cnayral@insa-toulouse.fr, fdelpech@insa-toulouse.fr, tricard@insa-toulouse.fr.*

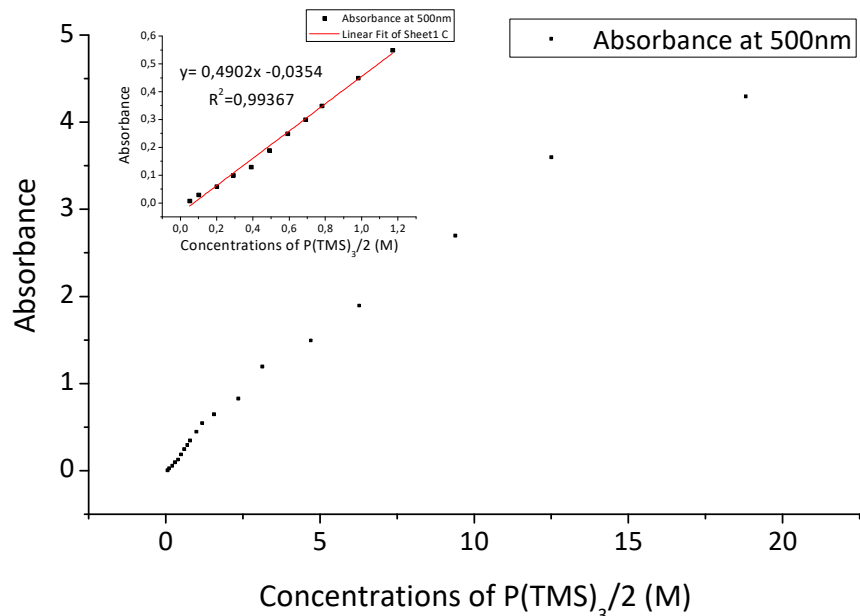


Figure S1. Evolution of the absorbance of Cd<sub>3</sub>P<sub>2</sub>@HDA QDs at 500 nm with the concentration of the limiting precursor introduced. Inset: zoom on the low concentration region

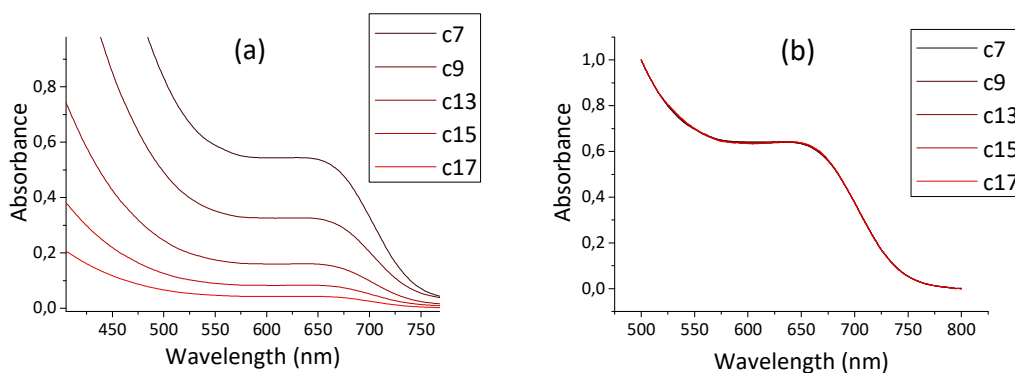


Figure S2. a) Absorption spectra of Cd<sub>3</sub>P<sub>2</sub>@HDA at different concentrations – b) Normalized curves

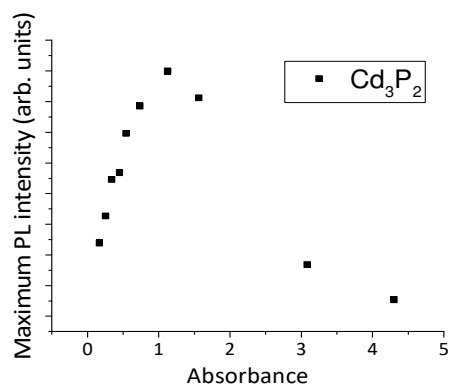


Figure S3. Evolution of the maximum PL intensity of Cd3P2 upon dilutions

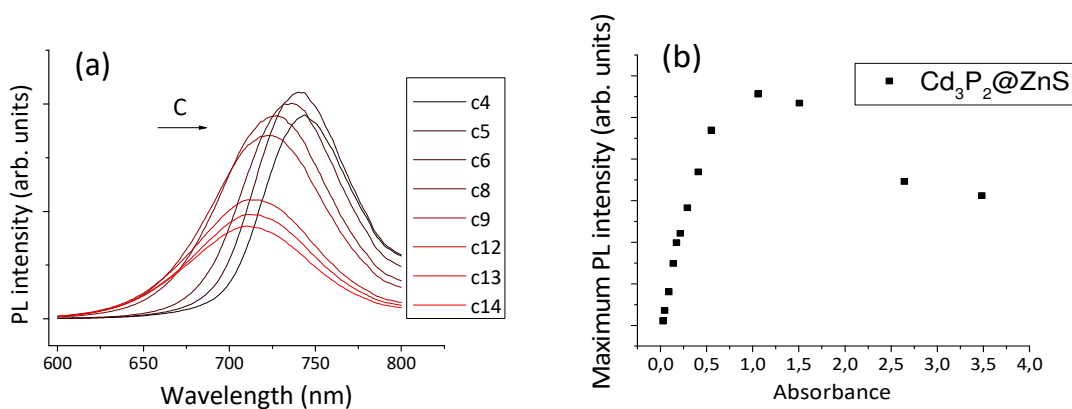


Figure S4. a) PL spectra of Cd<sub>3</sub>P<sub>2</sub>@ZnS and b) Evolution of the maximum PL intensity of Cd<sub>3</sub>P<sub>2</sub>@ZnS at different concentrations

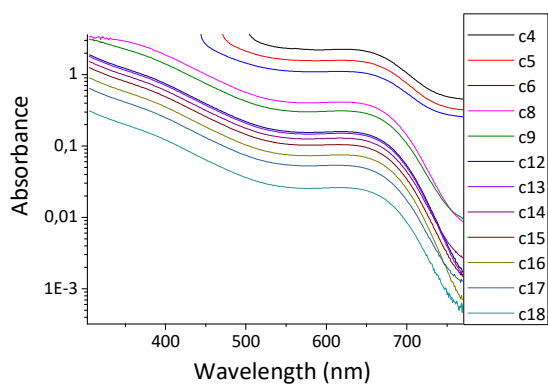


Figure S5. Absorption spectra of Cd<sub>3</sub>P<sub>2</sub>@ZnS solution at different concentrations

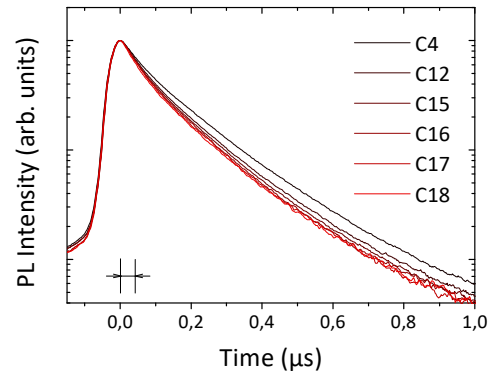


Figure S6. PL dynamics of  $Cd_3P_2@ZnS$  at several concentrations

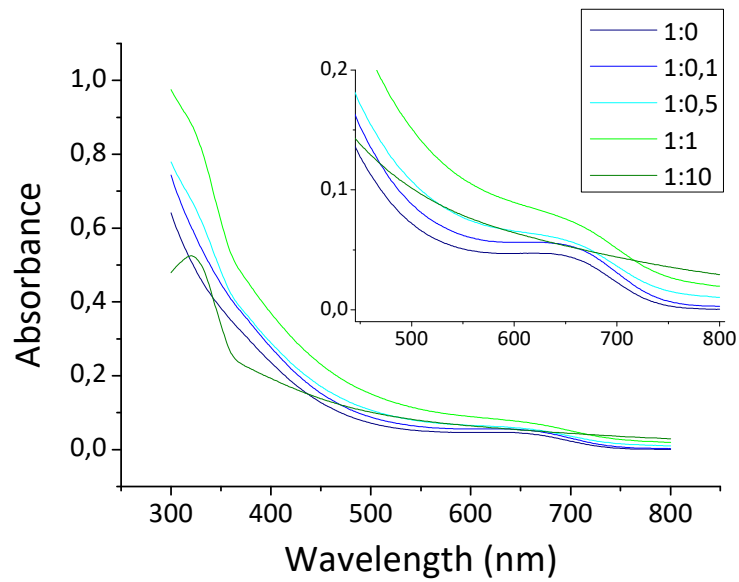


Figure S7. Absorption spectra of mixture of  $Cd_3P_2@OA$  and Pt NPs (legend : ratio  $Cd_3P_2@OA:Pt$  NPs).

*Inset: zoom on the 450-800 nm range*